Finite width of quasistatic shear bands

E. A. Jagla
Centro Atómico Bariloche, Comisión Nacional de Energía Atómica, (8400) Bariloche, Argentina
(Received 6 May 2008; published 8 August 2008)

I study the average deformation rate of an amorphous material submitted to an external uniform shear strain rate, in the geometry known as the split-bottom configuration. The material is described using a stochastic model of plasticity at a mesoscopic scale. A shear band is observed to start at the split point at the bottom, and widen progressively towards the surface. In a two-dimensional geometry the average statistical properties of the shear band look similar to those of the directed polymer model. In particular, the surface width of the shear band is found to scale with the system height H as H^{α} with $\alpha=0.68\pm0.02$. In more realistic three-dimensional simulations the exponent changes to $\alpha=0.60\pm0.02$ and the bulk profile of the width of the shear band is closer to a quarter of a circle, as it was observed to be the case in recent simulations of granular materials.

DOI: 10.1103/PhysRevE.78.026105 PACS number(s): 62.20.F−, 81.40.Lm

I. INTRODUCTION

Amorphous and granular materials have a strong tendency to develop localized deformation when submitted to shear deformation. This deformation concentrates usually in narrow regions, called shear bands. Upon a uniform rate of shear deformation, the material experiences a finite stationary deformation rate within the shear band, whereas the deformation rate is vanishingly small outside it [1,2]. In some cases the existence of strain localization can be associated to a decreasing form of the stress as a function of strain rate in the material. This decreasing leads to instabilities that drive the formation of shear bands.

An interesting limiting case corresponds to the so-called quasistatic shear banding. In this case the applied strain rate is vanishingly small, and the velocity field across the sample must change by a factor when there is a change of the driving force by the same factor. It seems that in this case a stationary, finite width shear band can only be obtained through the application of inhomogeneous conditions that break the uniformity of the system. In fact, simulations of homogeneous amorphous materials well below the glass temperature show the existence of shear bands which, however, thicken in time, eventually taking over the whole system [3].

A particular example in which the shear band is induced through the use of appropriate boundary conditions is the split-bottom container geometry introduced in [4,5] in the form of a modified Couette cell. In this configuration the bottom of the cell is split into two disks that rotate relatively to each other, and are attached to the inner and outer cylindrical wall of the cell. The sharp velocity interface at the bottom of the container induces an abrupt change of the velocity profile of the material close to this split line. Experiments using granular materials show that in these conditions the material inside the cell reaches (on average) a stable configuration in which the transition between particles moving rigidly with one or the other part of the bottom surface occurs in a transition zone that defines the shear band. The form of this zone is well defined and nonsingular even in the limit of "quasistatic" shear bands, i.e., when the relative velocity of both parts of the container is vanishingly small. However, when horizontal planes progressively away of the bottom are considered (and thus the influence of the split-bottom decreases), the width of the shear zone becomes larger, and no upper limit seems to exist. The width of the shear band starts as zero right at the bottom of the container, and progressively increases when moving upwards, being maximum at the free surface. The detailed study of the form of this profile is the subject of this paper.

The geometry that I will use here is a more symmetric version of the split-bottom experiment, which is depicted in Fig. 1. The bottom of the container defines the y-z plane, which is split along the $y=0$ line. The x direction is perpendicular to the bottom plane. The system is infinite in the z direction (in the three-dimensional numerical implementation, periodic boundary conditions along z will be used). The configuration is symmetric upon a change of sign of the y coordinate, and thus the center of the shear band is always located at $y=0$. Note that this applies to the *time averaged* position of the shear band, and not necessarily to an instantaneous configuration. We will come back to this fact in the discussions. This geometry has been introduced and studied in a continuum approach in [6], and analyzed numerically using frictional spherical particles in [7].

To predict, or justify, the form of the shear band we have to make assumptions about the structural response of the medium. One of the simplest starting points to model a plastic material is the assumption of "perfect plasticity." Under this hypothesis, each piece of material behaves elastically at small deformation, i.e., the stress is proportional to the strain, but if some threshold deformation is overpassed, the stress remains constant. It can be shown that if this simple prescription is followed, a singular shear band is obtained that goes from the split line at the bottom to the free surface at the top [8]. If the threshold deformation is uniform in the sample the shear band is a vertical plane above the split line, namely the y-z plane. However, if different thresholds are assigned to different points of the sample the shear band obtained is the homogeneous projection in the z direction of a wavy line in the x-y plane that goes between the split line at the bottom, and the free surface at the top. This shear surface can be obtained as the one that minimizes the energy generated as "heat of friction" during sliding.

In Ref. [9], Torok *et al.* put forward the idea that this minimal path is not persistent in time, since upon some re-

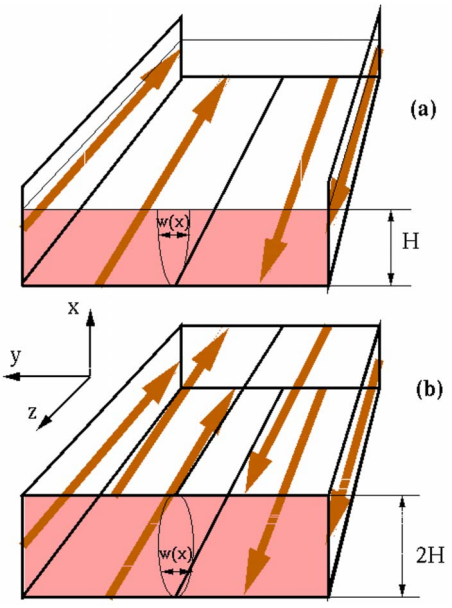

FIG. 1. (Color online) (a) The split bottom geometry. Left and right parts of the system are driven at a very small velocity v and $-v$, respectively. The top surface is free of force. The velocity of the material matches these values close to the bottom surface, and interpolates continuously in the bulk, as indicated schematically. (b) A split top-bottom geometry. Now the top surface is also split into two, similar to the bottom. Note the definition of the height H in both cases, which is made in this way to allow a better comparison. Even in the absence of gravity effects it is not obvious that the configuration in (a) should be equivalent to half of the configuration in (b), as it is explained in the text.

arrangement of the particles, the thresholds near the shearing surface are likely to change, and the path can move around slightly. In this way, a fluctuating path connecting the split point and free surface is obtained. It was thus suggested that the average configuration of this fluctuating path produces the continuum shear band observed in the experiments. Simulations based on the two-dimensional version of this idea (in which the z coordinate is eliminated, and the problem is solved in the x-y plane, assuming homogeneity along z) find a shear band that, after time averaging, is an object that widens from bottom to top.

An interesting magnitude that has been studied with some detail in this context is the scaling of the width w of the shear band at the surface as a function of the cell height H. In a reported experimental work [4] it was found that there is a power-law dependence for this quantity, with the shear band width w scaling as H^{α}, with α between 0.5 and 1.0. In the numerical work of Torok *et al.* [9], a value close to $2/3$ was found for α, and it was noticed that this is the analytical value known to occur in the case of directed polymers (DPs) in $1+1$ dimensions [10]. After this, it seems that people have taken the value of $2/3$ as a reference, and systematically try to scale the results of experiments or simulations with this value [11].

In my view there is not any strong reason why this should be the exact scaling exponent. The only point to be remarked is that the problem of DPs at zero temperature [10] is in essence very similar to the case of the fluctuating shear line in two dimensions. The main difference is that in the case of polymers the whole distribution of thresholds (and not only close to the shear line) is updated in every time step. The fluctuation of the tip of DPs at the surface of the system is analytically known to grow as $H^{2/3}$. However, the problem of the shear band is a continuous three-dimensional one, and this makes the comparison with the DP rather obscure.

Much less experimental information exists on the width of the shear band inside the material, namely $w(x)$, for $0<x<H$. This is in part originated in the difficulty to observe the movement of the particles in the bulk, although some advances have been made in this direction [12,13]. In Ref. [7], Ries *et al.* did numerical simulations using a rather realistic three dimensional model of spherical particles interacting through friction contact forces. I consider that the results in this work complement nicely the available experimental measurements. In these simulations, in addition to the (approximate) $2/3$ power scaling of $w(H)$, a quarter of a circle profile was adjusted for the width in the interior of the material, namely, $w(x) \sim \sqrt{x(2H-x)}$.

It would be interesting to compare these results with the equivalent ones obtained with the previously mentioned model of fluctuating shear lines [9]. Unfortunately, the results in Ref. [9] are not very detailed concerning the width across the whole sample. Coming to the problem of DPs, to my surprise I have not found a detailed study of the full profile either, and then I set up a simulation code to study this case too. The results obtained for DPs will be presented below.

The DP model, or the model of fluctuating shear line of Ref. [9] consider that instantaneously, the shear band connects the split-bottom point and the free surface by a single line that fluctuates in time. Experimentally, there is no evidence that this is the case. In fact, even for the lowest velocities that can be measured, the velocity profiles that are observed seem to be continuous. This is one reason to try some model which is a bit more realistic and considers the possibility of continuous deformations, both in time and space. Another reason to search for a more realistic model is the fact that the DP model, and the model of fluctuating shear line of Ref. [9] are eminently two dimensional, and cannot be easily generalized to three dimensions [14]. In fact, in three dimensions, an instantaneous slip surface cannot occur throughout the system, unless its profile is independent of the third (z) dimension. The problem of the width of a shear band we are discussing is really a three dimensional one. Although it can be investigated by two-dimensional models (defined in the x-y plane in Fig. 1), it is not clear if there are crucial issues associated to the third direction. In this sense, note that the problem is homogeneous in the z direction only on average, but not instantaneously due to the randomness of the material.

The model presented in this paper advances along these lines, it is defined in principle on a continuous space and can be implemented in three dimensions. It allows one to obtain accurate results of experimentally measured quantities, and it is a good benchmark to test other phenomenological approaches to this problem.

II. A MESOSCOPIC SCALE MODEL

The model studied here is a simplification over the model introduced in Ref. [15] to study the finite width of shear bands in the presence of structural relaxation. Here this structural relaxation will be absent. I consider a two-dimensional planar geometry. The main variables of the problem will be the out-of-plane displacement $u(x,y)$ (in-plane displacements are not allowed). The strain field is defined by the two-component vector $e_x=\partial u/\partial x$, $e_y=\partial u/\partial y$.

A perfectly elastic two-dimensional material with only out-of-plane degrees of freedom is thus modeled through the local free energy $f=B(e_x^2+e_y^2)$, where B is related to an elastic constant of the material. In order to model a plastic material, I introduce a plastic strain field e_i^{pl} $(i=x,y)$ in such a way that the local free energy reads

$$f(x,y) = B[(e_x - e_x^{pl})^2 + (e_y - e_y^{pl})^2]$$

$$F = \int f(x,y)dxdy. \tag{1}$$

The time evolution of $u(x,y)$ can be considered to be determined in the quasistatic limit by a relaxational first-order equation of the form

$$\frac{du(x,y)}{dt} = -\lambda \frac{\delta F}{\delta u(x,y)}. \tag{2}$$

The model must be complemented by the time evolution of the plastic strain. In principle, a totally deterministic model for the evolution of e_i^{pl} could be tried. For instance, we can postulate that if the local free energy exceeds some threshold value, the system adjusts its plastic strain in such a way that the energy remains below the threshold. However, all my attempts to implement this kind of fully deterministic model led in the present geometry to a singular slip surface, i.e., to a shear band of zero width. In order to obtain a shear band of finite width, the totally averaged, deterministic evolution does not seem to be enough, a stochastic component must remain [16]. There are different possibilities for the choice of the stochastic evolution, but I think the kind of results that are obtained is rather independent of the details. The model adopted here is the following. I start with a zero local plastic strain. Upon evolution according to Eq. (2), the strain field e_i changes, and also does the local energy f [Eq. (1)]. The plastic strain is fixed to zero until f overpasses some local threshold value $f_{th}(x,y)$, then the value of $e^{pl}(x,y)$ is set instantaneously to the value of $e(x,y)$. In this way the local free energy is relaxed to zero. In addition, a new random value of $f_{th}(x,y)$ is chosen. This accommodation of the plastic strain models the plastic events that occur in the system, which allow to produce a potentially very large deformation, by the application of a finite stress.

Some comments are necessary about the actual implementation of the model on a discrete lattice. I use a discrete square lattice, labeled by indexes m, n, in such a way that I have a finite set of variables $u_{m,n}$. In the absence of plastic field Eqs. (1) and (2) lead to an evolution equation for $u_{m,n}$ that involves the discrete Laplacian. The form usually adopted would be

$$\frac{du_{m,n}}{dt} = \lambda(u_{m+1,n} + u_{m,n+1} + u_{m-1,n} + u_{m,n-1} - 4u_{m,n})/a^2, \tag{3}$$

where a is the lattice parameter. This implementation of linear elasticity is known to give a fully rotational invariant description, as we aim to. However, in the presence of plastic fields we must first calculate the two components e_x and e_y of the strain field, subtract the plastic fields e_x^{pl}, e_y^{pl} and then take the divergence to implement Eqs. (1) and (2). If plastic fields are defined naively along the links of the square lattice, it is very easy to arrive to unnatural, very anisotropic results that reflect the structure of the underlying square lattice. Instead, I define the plastic fields on the plaquettes defined by the square lattice. The scheme is the following. At any time step I calculate the local strain field in each plaquette as

$$e_x = B(u_{m+1,n+1} + u_{m+1,n} - u_{m,n+1} + u_{m,n})/2a, \tag{4}$$

$$e_y = B(u_{m+1,n+1} + u_{m,n+1} - u_{m+1,n} + u_{m,n})/2a, \tag{5}$$

and the local free energy f in the plaquette is calculated according to Eq. (1). If f is lower than the corresponding f_{th} the local plastic fields are left untouched, but if f is greater than f_{th}, the local plastic fields are updated to become equal to the total deformation field, i.e.,

$$e_x^{pl} \leftarrow e_x, \tag{6}$$

$$e_y^{pl} \leftarrow e_y, \tag{7}$$

and a new threshold f_{th} is chosen. Although in principle this algorithm is not guaranteed to produce rotationally invariant results, the results obtained show that this is so to a reasonable accuracy. This is why I have used the model in this form, without introducing additional terms (that would slow down the simulation) to obtain rotationally invariant results.

III. RESULTS

A. Directed polymers

First of all I will present the results obtained using the DP model. As I mentioned before, this part should have been only a reference to the literature, but surprisingly, the results shown here have apparently not been presented before.

As a first check, I reproduced with high precision the analytical 2/3 power for the scaling of the width at the surface if the number of elements of the polymer is sufficiently large, as can be seen in Fig. 2. The full curve $w(x)$ of the largest polymer studied is also plotted in that figure. It coincides at the surface with the previous curve, by definition, but is systematically different in the bulk. To my knowledge, there is no analytical expression for the $w(x)$ profile of a DP. Note that the half-profile for a DP fixed at both ends (plotted also in Fig. 2) shows clear differences with the free end case: the width of the free end case is systematically larger than the fixed end case, they only coincide asymptotically close to the fixed point. Note also that the curve for the polymer with two fixed ends has clearly zero slope at the middle point,

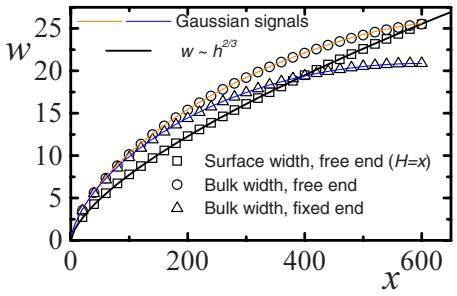

FIG. 2. (Color online) Squares: Numerical results for the average fluctuation of the free end of a directed polymer as a function of the number of its elemental pieces. The analytical 2/3 power (thick continuous) is very well reproduced once the number of elemental pieces becomes large. The full profile of a free end polymer (circles), and the half profile of a fixed end polymer (triangles) with $H=600$ are also plotted (for better visualization not all points are plotted). Continuous lines: fitting using the random Gaussian signals of Ref. [17] [Eq. (14)].

which is obviously due to symmetry reasons, but this is not obviously the case for the free end polymer.

To analyze these results in more detail, it turned out to be very successful to apply the theory of Gaussian signals developed in Ref. [17]. This consists in the study of the properties of a self-affine stochastic process, submitted to the appropriate boundary conditions, assuming a decomposition into uncorrelated Fourier modes of Gaussian amplitude. Although the hypothesis of the modes being uncorrelated is usually not satisfied, this analysis is known in particular cases to provide results that fit the exact data with high accuracy [18]. The simplest case to start with is that of the fixed ended polymer. In this case it is assumed that the stochastic process can be decomposed in Fourier modes in the form:

$$Y(x) = \sum_{n=1}^{\infty} g_n A_n \sin(n\pi x/2H), \tag{8}$$

where $Y(x)$ is the y coordinate of the polymer at height x (see Fig. 1), g_n are uncorrelated random numbers with zero mean and unitary variance, $2H$ is the distance between the two fixed ends of the polymer, and A_n is the amplitude of the corresponding mode. For self affine processes with scaling properties, the amplitudes A_n must scale as a power of n, namely $A_n = C_0 n^{-\gamma}$, where an H-dependent global constant C_0 was introduced. By multiplying and taking averages over realizations we obtain the statistical width w at distance x of one fixed end as

$$w^2(x) = C_0^2 \left(\sum_{n=1}^{\infty} n^{-2\gamma} \sin^2(n\pi x/2H) \right) \tag{9}$$

where I have made use of the fact that different g_n are uncorrelated. The exponent γ can be related to our exponent α for the expected scaling of the stochastic process at the surface. It is not difficult to show that $\alpha = \gamma - 1/2$. Thus we can write

$$w^2(x) = C_0^2 \left(\sum_{n=1}^{\infty} n^{-2\alpha-1} \sin^2(n\pi x/2H) \right). \tag{10}$$

As an example, note that the thermally fluctuating elastic line problem has $\alpha = 1/2$, and the sum in Eq. (10) gives

$$w(x) = \frac{\pi C_0}{2\sqrt{2H}} \sqrt{x(2H-x)}, \tag{11}$$

i.e., a half circle profile, that is the exact result in this case. For DPs we have $\alpha = 2/3$, and the result for $w(x)$, fitting the global factor C_0 is shown on top of the numerical results in Fig. 2 and cannot be distinguished from the numerical data.

Going to the case of the free end polymer, note that in the problem of thermally fluctuating elastic line, only modes that reach the surface with zero derivative must be considered. This leads to a profile of the form

$$w^2(x) = C_0^2 \left(\sum_{n\mathrm{Odd}} n^{-2\alpha-1} \sin^2(n\pi x/2H) \right), \tag{12}$$

where now the sum is over half the modes we had before. The result obtained scales as

$$w(x) \sim \sqrt{x}. \tag{13}$$

In particular, this profile does not have zero derivative at the surface, although it is constructed with modes that have zero derivative individually.

Coming back now to the free end DP, an attempt can be made to fit the curve of an open end polymer weighting appropriately the modes with zero value at the surface, and those with zero derivative, keeping the self-affine nature of both of them individually. This corresponds to a width function of the form:

$$w^2(x) = C_0^2 \left(\sum_{n}^{\infty} [1 - \beta(-1)^n] n^{-2\alpha-1} \sin^2(n\pi x/2H) \right). \tag{14}$$

The best fitting to the numerical results is obtained when we choose $\beta = 1/2$, and C_0 as the same value used to fit the fixed end case. The fitting, shown in Fig. 2, cannot be distinguished from the numerical results either. Note that having the same value of C_0 means that the asymptotic form of $w(x)$ for $x \to 0$ is exactly the same for the free end and open end situations [this is because the alternating in sign β term in Eq. (14) introduces for small x a contribution that is a larger power of x than the main term], which is observed to be very well satisfied numerically.

A very sensitive quantity that can be used to evaluate the results just presented is the local slope s of the $w(x)$ curve, defined as $s(x) = d \ln w(x) / d \ln x$. These results, both from numerics and using the fitting with Gaussian signals are shown in Fig. 3. Two facts must be noticed: first, for open end polymers, the slope vanishes at the surface as $(H-x)^{1/3}$ according to the Gaussian theory (and this is well reproduced by the numerics), more singularly than the linear vanishing of the fixed end case at the midpoint. Second, for $x \to 0$ is $w(x) \sim x^{2/3}$, the Gaussian theory gives $w(x) \sim x^{2/3}$, and numerical data seem to indicate that this is also the case for the

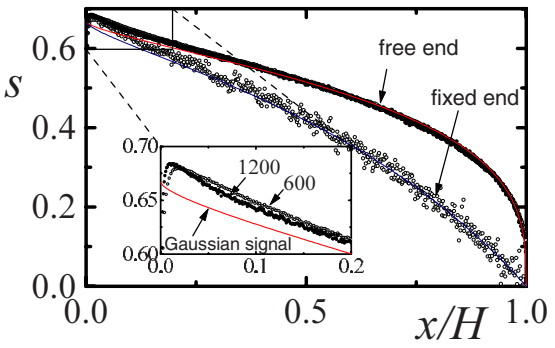

FIG. 3. (Color online) Logarithmic derivative of the bulk width data of free end DPs with $H=600$ and 1200, and fixed end DP with $H=600$, and the corresponding fitting according to random Gaussian signals (Ref. [17]). Note that for free end DPs, the derivative vanishes at the surface at $(H-x)^{1/3}$. Note also that the data for small arguments tend to approach the trend of the continuous line as size is increased, although very slowly (the blowup shows only data for the open end case).

DP model (although the convergence is slow with system size), i.e., the $x\to 0$ behavior has the same exponent than that of the surface scaling. This is a property of Gaussian signals but to my knowledge it is not obvious for DPs. I will come back to the meaning of this fact in the last section.

At present, I do not have any explanation that justifies the accuracy of the fitting proposed, and neither an explanation for the remarkably value of β obtained in the fitting of the open end polymer. The results just presented for DPs will serve as a reference for comparing those obtained with the mesoscopic plastic model.

B. Mesoscopic model: two dimensions

In a first stage, I implemented the mesoscopic model presented in Sec. II on a two-dimensional rectangular geometry corresponding to the x-y plane in Fig. 1, in which the border of the right half is given some velocity v, and the border of the left half is given the opposite velocity $-v$. The value of v is set small enough for the total velocity field to be simply proportional to this value.

Results for two different boundary conditions will be presented, depicted in Fig. 1. They correspond to the so-called split bottom geometry, Fig. 1(a), in which the top surface is left free, namely a condition of zero normal stress is applied, and the split top-bottom geometry, Fig. 1(b), in which the top plane is given the same boundary condition that the bottom plane. Note that although I use the expressions "top" and "bottom" to agree with the experimental device, in the present case I do not include a gravitational field that singles out a vertical direction. This choice is made as the numerical simulations in Ref. [7] indicate that gravity plays only a minor role in the structure of the shear band [19]. Simulations were performed for different values of the total height of the system H, and in each case the system size along the y direction was chosen sufficiently large for the shear band not to be affected by the lateral walls (typically, the size along y is around ten times the expected value of w at the surface).

Starting from rest, with both e_i and e_i^{pl} set to zero, the simulation is initiated by applying a finite velocity $\pm v$ to the left and right borders. At the first stages of the simulation, the system is seen to respond elastically, since in no place the value of f_{th} is overpassed. At some moment, f_{th} is overpassed for the first time in some place, the corresponding value of e_i^{pl} is changed as explained in Sec. II, and this feeds back to modify the evolution of e_i. After many plastic events at different spatial positions, the system reaches a stationary state (on average, since stochastic fluctuations of the plastic strain remain), and at this stage statistics can be accumulated to obtain the average velocity field. In the simulations presented, the threshold values f_{th} are chosen randomly in the interval $0.5\, f_{th}^0 < f_{th} < 1.5\, f_{th}^0$ where f_{th}^0 is a reference value. Dimensionless units are set by taking $f_{th}^0 \equiv 1$ and $\lambda B \equiv 1$ in Eqs. (1) and (2), and the lattice parameter $a \equiv 1$. In these units, the small velocity used to drive the system is 10^{-4}, and the time step is 0.1.

Note that all the distances in the model are measured in units of the lattice parameter a. In particular, the scaling of the shear band width at the surface $w(H)$ as $w(H)\sim H^\alpha$ can be written after reinserting a as $w(H)/a \sim (H/a)^\alpha$, or $w(H) \sim H^\alpha a^{1-\alpha}$. Our a plays a similar role than the particle size in experiments, as both set roughly the minimum size of a region where an independent plastic event can occur. In the model presented here, an additional, weaker dependence of w exists on the value of the dispersion chosen for the thresholds. As I explained before, as this dispersion goes to zero w goes to zero also, but as soon as this dispersion is a few percents or higher, the results for w depend weakly on it. I will not refer to this dependence further in this work.

The shear band forms as an effect of the sequence of plastic events in which the values of e_i^{pl} are adapted at different points in space. Although the plastic threshold are totally uncorrelated, the elastic field generates an overall tendency for plastic deformation to become correlated. In fact, a plastic slip occurring at some position (x,y) reinforces the possibility of a similar event occurring above or below, at the same y coordinate, and displaced in the x direction. However, the stochastic nature of the model makes this overall tendency not to be strict. Accumulated plastic deformations over progressively larger periods of time, shown in Fig. 4, allow one to understand the mechanics of the process. On very short time scales [Fig. 4(a)], almost individual events at isolated positions are observed. At intermediate time scales [Figs. 4(b) and 4(c)], we see how these events correlate in space to generate a sort of finite length shear lines. Note however that contrary to the fluctuating shear line model, here the plastic deformation does not accumulate at a single shear line, irrespective of the time interval considered. For the largest time scales [Fig. 4(d)] we can see the tendency for the fluctuating behavior to be averaged out, and for sufficiently large time intervals we obtain eventually a well-defined continuous shear band.

Now I will focus on the properties of the averaged shear band in this stationary situation. In Fig. 5(a) I plot the full profile for the width w of the shear band obtained in systems of different heights H. These data can be very well scaled if plotted as w/H^α against x/H. This is basically the same result obtained in experiments and in other simulations, ex-

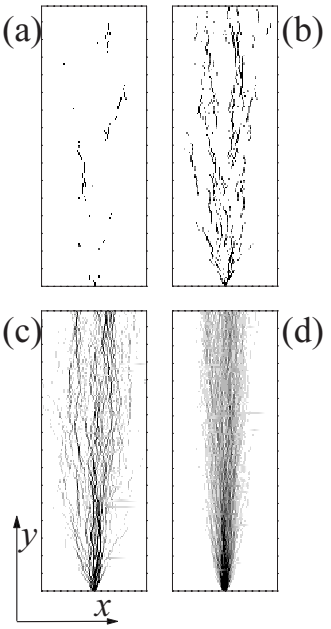

FIG. 4. Schematics of plastic deformation in the horizontal direction ($\partial u/\partial x$) accumulated over progressively larger periods of time Δt, namely, $\Delta t = 10^2$, 10^3, 10^4, and 1.5×10^5, from (a) to (d). Darker regions indicate zones with larger accumulated plastic deformation. Note that the plastic events appear at rather isolated positions (a), that then merge to generate pieces of shear lines (b) and (c). Over very large periods of time the fluctuating behaviors averages out, and a stationary, continuous shear band is observed (d).

tended here to the full profile inside the sample. The best fitting for the power α gives $\alpha = 0.68 \pm 0.02$ [see Fig. 5(b)]. Applying to this case the fitting using Gaussian signals, we obtain the fitting shown in Fig. 6. This is obtained using

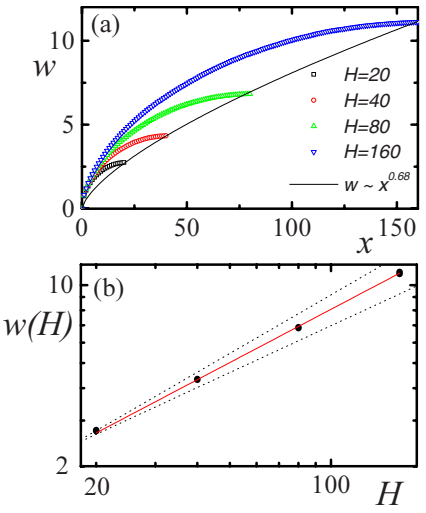

FIG. 5. (Color online) (a) Full profile of the width of the shear band across the sample for samples of sizes $H = 20$, 40, 80, 160 (symbols from bottom to top). (b) Evolution of the value of w at the surface with system size. The error bar is smaller than symbol size. The continuous line is the best fitting, with an exponent 0.68. Dotted lines have slope 0.60 and 0.75, for comparison.

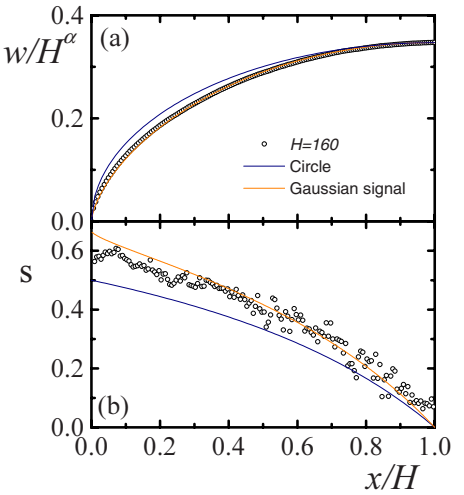

FIG. 6. (Color online) (a) The results of the previous figure scaled using an exponent $\alpha = 0.68$. The fitting using Gaussian signals and a quarter of circle profile are shown. (b) Logarithmic derivative of the data in (a), and the corresponding curves from Gaussian signals and for a circle.

expression (14) with $\alpha = 0.68$ (taken from the surface scaling), and $\beta = 0$. The corresponding logarithmic derivative of the data and the fitting are shown also in Fig. 6(b). Although a slightly different from zero value of β gives a somewhat better fitting, I think it is within the numerical uncertainty. The plot of the logarithmic derivative of the data [Fig. 6(b)] shows that the form of the curves close to the fixed point may correspond, in the large system size limit, to have the same exponent as the one of the surface scaling.

Note that the $\beta \sim 0$ value for the free surface case means that probably in the present model there are not significant difference between the split bottom and split top bottom geometry of double size. To confirm this fact, in Fig. 7 I show the results for the split bottom, and split top-bottom configuration with $H = 80$, where it can be seen than there are not any significant differences between the two. This results was not obvious from the beginning, since the symmetry of the split top-bottom geometry with respect to the horizontal middle plane exists only on average, and not instantaneously. The present finding agrees with the observation in Ref. [7] of a profile that hits the surface with zero derivative (in that

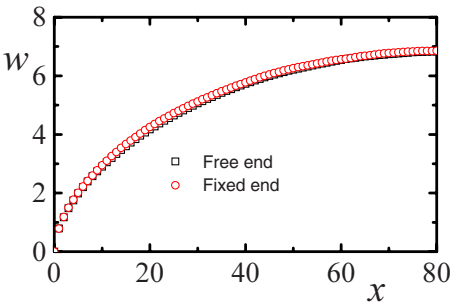

FIG. 7. (Color online) Comparison between the profile obtained for a split bottom configuration (free end case), and a split top-bottom configuration (fixed end case), for $H = 80$. No systematic differences can be observed within the numerical errors.

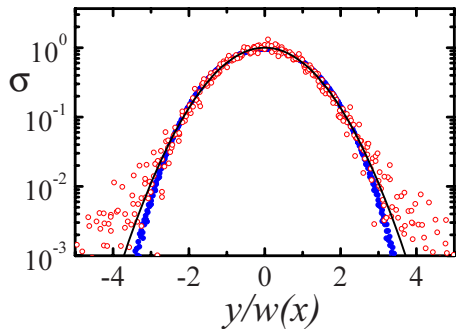

FIG. 8. (Color online) Derivative of the velocity profile $\sigma(y) \equiv dv(y)/dy$ for the directed polymer (full symbols) and the plastic mesoscopic model (open symbols). Data at $x=H/4$, $x=H/2$, $x=3H/4$, an $x=H$ are put all together by scaling the y axis with the corresponding values of the width w. The deviation of DPs from a Gaussian (in defect for large values of x) is clearly visible. The quality of the data for the plastic model is not sufficient to make a statement about deviations with respect to a Gaussian.

work however, it was not checked that the full profile was identical to half profile of a split top bottom case with double size). In Ref. [7] it was also observed that the full profile of the $w(x)$ could be nicely fitted with a quarter of a circle profile. An attempt to do this in the present case shows (see dashed line in Fig. 6) apparent differences between this function and the numerical data that seem to be much larger than those reported in [7]. I will come to this attempt of fitting in the next section.

In addition to the plot of the width of the shear band, it is interesting to evaluate the full profile of the velocity at some typical vertical position, i.e., to consider the velocity $v(y)$ at some fixed value of x. Numerical and experimental results show that to a good approximation this profile can be fitted by an error function. The experimental data in [5] show excellent agreement with an error function at least up to the point where velocity has decay to approximately 10^{-6} with respect to the maximum. On the other hand, the numerical simulations in [7] show profiles that go above the error function when this takes values below approximately 10^{-3}. It is not totally clear however if this difference will persist in infinitely long runs, as the difference slightly reduces as the simulation time increases.

Given the velocity profile $v(y)$ at some fixed x position, its y derivative will show a Gaussian form. This quantity, noted $\sigma(y)$ is presented in Fig. 8 for the mesoscopic model, and for DPs. Data at the surface of the system, and in some particular positions in the bulk are included to show that there are no systematic differences between surface and bulk. The y axis is scaled in each case by the corresponding value of $w(x)$, and the normalization $\sigma(0)=1$ is used, in such a way that the best Gaussian fitting is given in all cases by the function $\exp(-x^2/2)$. The results for DPs fall clearly below the Gaussian fitting for sufficiently large values of the argument, namely in the tail of the distributions. This is a well-known result. Results for the mesoscopic model indicate a good Gaussian fitting for $|y| \lesssim 2w(x)$. Data seem to indicate a slight deviation in excess for larger values of y. However, these result require more massive simulations to be confirmed.

C. Mesoscopic model: three dimensions

The results of the previous section indicate that the two-dimensional mesoscopic model has similarities and differences with the fluctuating shear line, or the DP model, and with results of other kind of simulations [7]. In particular, the result obtained for the exponent $\alpha=0.68\pm0.02$ is remarkably consistent with the analytical $2/3$ exponent of DPs. Experimentally, the obtained exponent is consistent with a $2/3$ value, but to my knowledge a fitting of this exponent from the experimental results has not been attempted, and probably values within ±0.1 of $2/3$ will be equally consistent with the experiments.

However, an important point of discrepancy between the present results and atomistic numerical simulations in Ref. [7] is the form of a quarter of a circle profile found there for $w(x)$. The results of the previous section (see Fig. 6) seem to depart from this behavior in a larger extent than the results in [7].

One of the possible reasons for this discrepancy is the fact that the results in [7] and experiments in general are fully three dimensional, while all the results presented up to now here are two dimensional. It is important to emphasize that although in the geometry studied there is translation symmetry *on average* along the z direction, the stochastic nature of the problem implies that fluctuations are not invariant along this direction. Actually, the setting up of a model that can be implemented in three dimensions was one of the motivations of the present research.

A full implementation of the mesoscopic plasticity model in three dimensions requires the use of a three component displacement field $u_i(x,y,z)$, $i=x,y,z$. This presents some technical challenges that I have not overcome yet. However, a partial implementation of the three-dimensional case is possible, and the results obtained are already very interesting.

The idea is to keep working with a single component displacement field u which is the displacement along z direction, keeping $u_x=u_y=0$. The model can thus be described as a collection of planes in which a set of equivalent two-dimensional problems are defined, and where the plastic thresholds are chosen independently for each plane. The fundamental variable is then some $u(x,y)_i$ where index i labels the plane along the z direction. Planes are connected to nearest neighbor ones by purely elastic forces, in such a way that the total energy of the system is now

$$F = \sum_i \left(F^i + \frac{k_z}{2} \int dxdy (u_i - u_{i+1})^2 \right) \tag{15}$$

where F^i is the previous two-dimensional free energy for plane i. Periodic boundary conditions are applied along z. The size of the system along z should be chosen large enough. To keep a consistent implementation, this size is always chosen to be equal to the total thickness H of the system. The coupling constant k_z along z is chosen to be equal to the linear elastic constant within the plane. Note that no plastic threshold is implemented for the springs along z. This version of the model was simulated in exactly the same manner as the two-dimensional case. The results for the

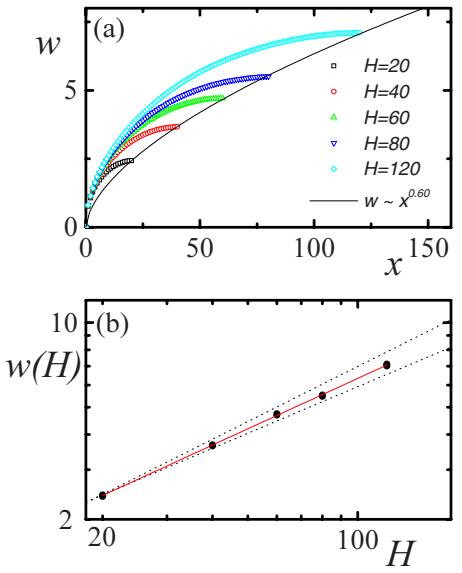

FIG. 9. (Color online) (a) Three dimensional data for samples with $H=20$, 40, 60, 80, 120 (symbols, from bottom to top). (b) Evolution of the value of w at the surface with system size. The error bar is smaller than symbol size. The continuous line is the best fitting, with an exponent 0.60. Dotted lines have slope 0.55 and 0.65, for comparison.

width function $w(x)$ for systems of different sizes are shown in Figs. 9 and 10. Data for different values of H can again be scaled by plotting w/H^{α} vs w/H. The fitting of α gives $\alpha=0.60\pm0.02$.

Two important differences appear between the three-dimensional and the previous two-dimensional simulations. First of all, the scaling of data for systems of different thickness is obtained using an exponent smaller than that of the two-dimensional case, namely $\alpha^{3D}\sim0.60$, $\alpha^{2D}\sim0.68$. The precision of the present simulations allows one to claim that

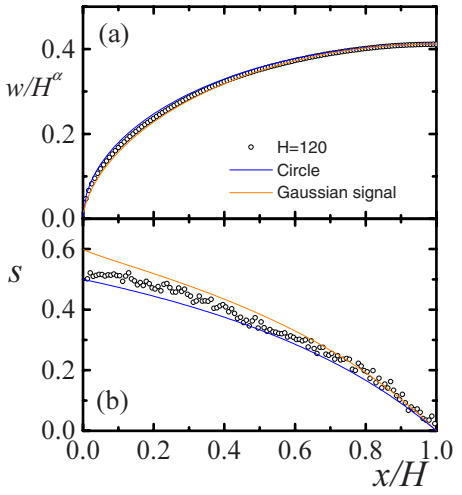

FIG. 10. (Color online) (a) The data of the previous figure corresponding to the largest system size ($H=120$) are shown together with a fitting using Gaussian signals with exponent 0.60 and a quarter of circle profile. (b) Logarithmic derivative of the data in (a), and the corresponding curves from Gaussian signals and for a circle.

this difference is significant. In my view other numerical simulations or experiments have not reached yet the point to tell the growing exponent with a precision of ±0.1. I think a value close to 0.6 is consistent with the precision of accessible experimental results. More experimental work is needed concerning this point. The second difference between two and three dimensions is the overall shape of the $w(x)$ function. The form of this function in three dimensions is much closer to a quarter of circle profile (see Fig. 10). This may be an interesting observation when comparing with the results in [7], for instance. However, I have to mention that the fitting to this functional form does not seem to improve as the system size is increased, systematic differences apparently exist.

Related to this behavior, there is an interesting point to emphasize. Given a set of curves $w(x)$ for different thicknesses H, if the H dependence can be absorbed by a single-parameter rescaling, we must have

$$w(x)=w_0(y/H)H^{\alpha} \tag{16}$$

where w_0 is an H-independent function. If we assume w_0 behaves as a power law (with exponent α') for small values of its argument, we have

$$w(x\to0)\sim(x/H)^{\alpha'}H^{\alpha}=x^{\alpha'}H^{\alpha-\alpha'}. \tag{17}$$

Note that unless $\alpha=\alpha'$, the behavior of w close to the origin will depend on the value of H, no matter how large this is. In particular, $w(x\to0)$ will increase without limit (if $\alpha>\alpha'$) or decrease to zero (if $\alpha<\alpha'$) as H increases. This would be in my view a very strange behavior, although I have no rigorous argument against it. The DP curves shown in Figs. 2 and 3 are in fact compatible with a 2/3 power close to the fixed point, and for the two-dimensional plastic mesoscopic model a value of $\alpha'=\alpha$ seems to be compatible with data in Figs. 5 and 6. The situation is less clear in the three-dimensional case. The value of α was found to be around 0.60. However, the value of α' from Fig. 10 seems to be consistently closer to 0.5 (which, by the way, is why the quarter of circle profile is accurate). It is not clear if the two exponents will show a tendency to become closer in larger system size simulations of if they will remain different.

IV. SUMMARY AND CONCLUSIONS

In this paper I presented results obtained for the "split-bottom" geometry using a mesoscopic model for the plasticity of an amorphous material. Two- and three-dimensional results were reported. In particular, the exponent for the width w of the shear band at the surface of the system for two dimensions was found to be 0.68 ± 0.02, comparable with the analytical 2/3 exponent obtained for directed polymers. In three dimensions the exponent was found to be somewhat lower, namely 0.60 ± 0.02. I want to recall, however, that the implementation of the three-dimensional case was only partial, and a full modeling would be necessary to verify if this value remains valid under a complete implementation. In two dimensions, the full profile of the width in bulk $w(x)$ was found to be well described by a random

Gaussian signal, and in particular it was found that no systematic differences appear between a system with a free top surface and system with a split surface at the top. This was not an obvious point from the beginning as the reference system for this study, namely the directed polymer, shows systematic differences between the two cases that I have addressed and described in terms of the theory of random Gaussian signals. In three dimensions, it was observed that the form of $w(x)$ can be fitted reasonably well by a quarter of circle profile, a result that has been obtained in previous work in a related model [7]. A caveat about whether this scaling can continue to be valid for arbitrarily large systems was put forward.

The number of experimental results that the present model describes, added to the very simple ingredients on which it is constructed, places it as a good candidate in which the deep origin of the regularities emerging from experiments can be elucidated. One promising route would be trying to generate continuous differential equations that describe the evolution of probability densities of the stochastic model. This is an interesting prospect for future work. Another route would be the investigation using this kind of model of more complex geometries where novel phenomena can be expected.

ACKNOWLEDGMENTS

Fruitful discussions with A. Kolton, A. Rosso, M. Falk, W. Losert and T. Unger are greatly acknowledged. This research was financially supported by Consejo Nacional de Investigaciones Científicas y Técnicas (CONICET), Argentina. Partial support from Grants No. PIP/5596 (CONICET) and No. PICT 32859/2005 (ANPCyT, Argentina) is also acknowledged.

[1] J. Duran, *Sand, Powders and Grains* (Eyrolle, Paris, 1997).
[2] R. Nedderman, *Statics and Kinematics of Granular Materials* (Cambridge University Press, Cambridge, UK, 1992).
[3] Y. Shi, M. B. Katz, H. Li, and M. L. Falk, Phys. Rev. Lett. **98**, 185505 (2007).
[4] D. Fenistein and M. van Hecke, Nature (London) **425**, 256 (2003).
[5] D. Fenistein, J. W. van de Meent, and M. van Hecke, Phys. Rev. Lett. **92**, 094301 (2004).
[6] M. Depken, W. van Saarloos, and M. van Hecke, Phys. Rev. E **73**, 031302 (2006).
[7] A. Ries, D. E. Wolf, and T. Unger, Phys. Rev. E **76**, 051301 (2007).
[8] T. Unger, J. Torok, J. Kertesz, and D. E. Wolf, Phys. Rev. Lett. **92**, 214301 (2004).
[9] J. Torok, T. Unger, J. Kertesz, and D. E. Wolf, Phys. Rev. E **75**, 011305 (2007).
[10] Y. C. Zhang and T. Halpin-Healy, Phys. Rep. **254**, 215 (1995).
[11] D. Fenistein, J. W. van de Meent, and M. van Hecke, Phys. Rev. Lett. **96**, 118001 (2006).
[12] K. Sakaie, D. Fenistein, T. J. Carrol, M. van Hecke, and P. Umbanhowar, e-print arXiv:0704.3745.
[13] X. Cheng, J. B. Lechman, A. Fernandez-Barbero, G. S. Grest, H. M. Jaeger, G. S. Karczmar, M. E. Mobius, and S. R. Nagel, Phys. Rev. Lett. **96**, 038001 (2006).
[14] Although the problem of directed polymers can be easily generalized to 2+1 dimensions, its relevance to the shear band problem is much less obvious in this case.
[15] E. A. Jagla, Phys. Rev. E **76**, 046119 (2007).
[16] Once the stochastic model is defined, one can try to obtain from it a smooth differential equation that describes the evolution of probability density in the stochastic model. This is similar to obtaining the Fokker-Planck equation from a Langevin dynamical equation. In the present case I have no clues on how to obtain this effective equation. This is a very interesting issue to pursue in the future.
[17] A. Rosso, W. Krauth, and R. Santachiara, J. Stat. Mech.: Theory Exp. (2005) L08001; R. Santachiara, A. Rosso, and W. Krauth, *ibid.* (2007) P02009.
[18] P. Le Doussal and K. J. Wiese, Phys. Rev. E **68**, 046118 (2003).
[19] Note however that other people [6,20] have suggested that the very origin of the shear band widening phenomenon lies in a dependence of a friction coefficient on the angle between local velocity gradient and the vertical line, i.e., gravity is of crucial importance in this interpretation. Since the origin of the effect is totally different in the model I am presenting I will not compare further my results with those in [6,20].
[20] M. Depken, J. Lechman, M. van Hecke, W. van Saarloos, and G. C. Grest, Europhys. Lett. **78**, 58001 (2007).